

Review Article

Nonadiabatic electron–phonon effects in low carrier density superconductors

E. Cappelluti^{*,1,2} and L. Pietronero^{1,2}

¹ INFM and Istituto dei Sistemi Complessi del CNR, v. dei Taurini 19, 00185 Rome, Italy

² Dept. Physics, University of Rome “La Sapienza”, P. le Aldo Moro 2, 00185 Rome, Italy

Received 24 September 2004, revised 3 November 2004, accepted 4 November 2004

Published online 6 December 2004

PACS 63.20.Kr, 71.20.Tx, 74.70.Ad, 74.72.–h

Different families of unconventional superconductors present a low charge carrier density as a common trait, suggesting that the low charge density can be at the basis of a unifying picture for different superconductors. In the past years we have suggested that the electron–phonon interaction can be responsible for a high- T_c superconducting pairing in a nonadiabatic regime, where nonadiabatic effects are triggered on by the small electronic Fermi energy associated with the low charge density character. A coherent picture of such a framework requires however reconciling the low charge density and the small Fermi energy with a finite metallic character (sizable density of states and large Fermi surfaces). In this paper we investigate the peculiar conditions which are needed to be encountered in order to fulfill these requirements. We discuss the specific case of fullerenes, cuprates and MgB_2 alloys by analyzing their specific structural and electronic properties. The comparison between these materials and simple instructive models permits to underline the different routes to reconcile these characteristics in different compounds. In cuprates and fullerenes the interplay between small Fermi energies and large Fermi surface is strictly connected with strong electronic correlation effects. A comprehensive understanding of these issues can be useful to the future search for new nonadiabatic high- T_c materials.

© 2005 WILEY-VCH Verlag GmbH & Co. KGaA, Weinheim

Contents

- 1 Introduction**
- 2 Low carrier density systems: bad metals or good superconductors?**
 - 2.1 A look at conventional metals
 - 2.2 Playing with parameters in conventional metals
- 3 Complex models for unconventional superconductors**
 - 3.1 Fullerenes and molecular crystals
 - 3.2 Cuprates and correlation effects
 - 3.3 MgB_2 and diboride alloys
- 4 Conclusions**

References

* Corresponding author: e-mail: emmcapp@roma1.infn.it, Phone: +0039 06 4991 3450, Fax: +0039 06 4463158

1 Introduction

For many years the concept of superconductivity has been strictly associated with the electron–phonon interaction. One of the fingerprints of the Migdal–Eliashberg theory in conventional *low* temperature superconductors has been in fact the prediction and observation of many peculiar features which are a direct evidence of a phonon mediated superconductivity, for instance the isotope effect α_{T_c} on the critical temperature, the extraction of the electron–phonon (el–ph) coupling function $\alpha^2 F(\omega)$ from tunneling experiments, phonon anomalies occurring at temperature $T = T_c$, etc. [1]. The belief that superconductivity was intimately related to an electron–phonon pairing was so strong that a semi-empirical upper limit for the critical temperature $T_c^{\max} \approx 20–25$ K ($T_c^{\max} \sim 40$ K in the pioneering work by McMillan [4]) was thought to be valid before the occurrence of lattice instabilities [2, 3], in agreement with the maximum $T_c \approx 23$ K achieved in Nb₃Sn.

This phonon-based scenario was shaken in 1986 by the discovery of high- T_c superconductivity in copper oxides [5] with T_c 's up to 140 K, well above the empirical limit $T_c^{\max} \sim 20–25$ K. In addition, the isotope effect on the critical temperature at the optimal doping δ_{opt} in cuprates was found to be unconventionally small $\alpha_{T_c} \lesssim 0.1$ [6], in agreement with a non phonon mediated mechanism. Following this perspective a large amount of work has been devoted in the two last decades to the study of purely electronic models to explain the high- T_c superconductivity.

In the recent years however, the evidence of an important role of the electron–phonon interaction on many properties of the normal and superconducting state has been increasing. On one hand, the small value of α_{T_c} turned out to be a peculiarity of the optimal doping, whereas in the underdoped region α_{T_c} could be significantly larger, even higher than the BCS limit $\alpha_{T_c} = 0.5$ [7, 8]. On the other hand a remarkable isotope effect on the zero temperature London penetration depth $\lambda_L(0)$ has been observed both in the nearly optimal and in the underdoped regime [9–11]. The finite isotope shift on $\lambda_L(0)$ has been related to an isotope effect on the effective electron mass m^* through the relation $\lambda_L(0) = \sqrt{n_s/m^*}$, where n_s is the superfluid density. The observation of a finite isotope effect on $\lambda_L(0)$ or on m^* is highly puzzling since these quantities are expected to show *strictly zero* isotope effect in the conventional electron–phonon framework. The report of a finite isotope effect on m^* can be thus regarded not only as an indication of an important role of the electron–phonon coupling, but also as an evidence of the unconventional nature of the el–ph interaction [12–15]. Further support to a significant electron–phonon coupling in cuprates comes from angle-resolved photoemission spectroscopy (ARPES). The kink of the electronic dispersion observed by these measurements was indeed claimed to be of phononic origin, since it shows a negligible dependence on doping, on temperature and on the angle direction along the Fermi surface [16, 17].

Motivated by this experimental scenario, there is nowadays a revamping interest about an unconventional role of the electron–phonon interaction in cuprates and its relation with superconductivity. The observation of high- T_c superconductivity with critical temperatures up to $T_c^{\max} \sim 40$ K in fullerenes [18–21] and in the recently discovered MgB₂ [22], where the phononic origin of the superconducting pairing is widely accepted, points out that a phonon-based mechanisms can be actually a route for high- T_c superconductivity, and it suggests a common mechanism for all these compounds.

An extremely low density of charge carrier is one of the characteristic features which is shared by cuprates, fullerenes and MgB₂, where the key role for superconductivity is played by the few carriers of the σ bands [23, 24]. This is quite surprising since low carrier density is an unfavorable element for superconductivity within the conventional framework of BCS or Migdal–Eliashberg theories. Moreover a small superfluid density, when not in the presence of additional charges not involved in the Cooper pairing (such as the π -states in the case of MgB₂), is unavoidably related to poor screening and to strong electronic correlations, ingredients which are expected to be also detrimental for conventional superconductivity. On these grounds it is hard to understand why these low carrier materials are the best superconductors.

The investigation of unconventional electron–phonon features beyond the standard Migdal–Eliashberg phenomenology has attracted a considerable interest even before the discovery of high- T_c

superconductors. Particular efforts have been devoted to the study of electronic and lattice properties in the polaronic and bipolaronic regime [25–28]. Polaron and bipolaron concepts [29–32], as well as anomalous features arising from lattice modulations (stripes) or instabilities [33, 34], have been also employed to analyze phenomenology of the high- T_c compounds.

In the past years we have proposed that nonadiabatic effects could be responsible for the high- T_c superconductivity in these compounds in the context of an unconventional phonon-based mechanism [35–39]. Nonadiabatic effects arise when the Fermi energy is small enough to be comparable with the phonon frequencies ω_{ph} : $E_F \sim \omega_{\text{ph}}$ [40]. The active principle in this theory is thus the opening of nonadiabatic channels of interaction which give rise to a complex electron–phonon phenomenology. The superconducting pairing, in particular, results to be strongly dependent on the *sign* of the nonadiabatic scattering, which leads to an effective enhancement or suppression of T_c . In this framework the superconducting properties are highly sensitive to specific material-dependent details, such as the electron filling n , the onsite Coulomb repulsion U , the effective Thomas–Fermi screening $\tilde{\kappa}_{\text{TF}}$, etc. Concerning the superconducting pairing, specific elements which favour high- T_c superconductivity were shown to be for instance: *i*) the strong electronic correlation which mainly selects the phase space (small momentum scattering) where nonadiabatic effects lead to an *enhancement* of the superconducting pairing, and thus it favors high- T_c superconductivity [35–37]; *ii*) the presence of a two-dimensional Van Hove singularity, which enhances the nonadiabatic degree of the system because of the flat bands at the saddle point and which enforce small momentum scattering *within* the saddle point [41, 42]; *iii*) the closeness of the band edge in two-dimensional systems [43, 44].

The generalization of the electron–phonon theory in the nonadiabatic regime can be best dealt with in terms of Quantum Field Theory which is usually discussed by means of Feynman’s diagrams. In this context the active principle of the high- T_c superconductivity is the opening of nonadiabatic channels in the electron–phonon interaction. It is worth to underline that the development of this approach has been mainly aimed to describe the onset of anomalous Fermi liquid properties within an (unconventional) *metallic* regime. In this sense it is qualitatively different and complementary to the polaronic scenario which becomes exact in the extremely anti-adiabatic (Lang–Firsov) limit [45] and which described self-trapped non-metallic polarons in the adiabatic limit.

Aim of the present paper is to discuss at a text-book level the physical conditions which determine the onset of the nonadiabatic effects and their consequences on basic physical properties. A rigorous derivation of the explicit equations of the nonadiabatic electron–phonon theory is thus out of the purposes of this paper and we refer the reader to Refs. [35–37, 41–44, 46–49] for more details on this subject.

2 Low carrier density systems: bad metals or good superconductors?

As above mentioned, a fundamental role in the high- T_c compounds is played by their small density of charge carriers n : small n implies small Fermi energies E_F which give rise to nonadiabatic effects as soon as $E_F \sim \omega_{\text{ph}}$. A low density of charge carriers involved in the Cooper pairing appears thus a natural by-product of nonadiabatic materials. This consideration calls however for further argumentations. According to this view indeed semiconductors, which are the simplest examples of systems with low, even vanishing, Fermi energy, should appear as the best candidates for high- T_c superconductivity. Of course, things are not so easy and high temperature superconductors are less common in nature than what expected by this argument alone. On the theoretical side one should consider that dimensionality plays an important role in common semiconductors: for small carrier densities the electronic dispersion close to the bottom of the conduction band (top for hole conductivity) can be approximated in the most cases with a three-dimensional free-like dispersion $\varepsilon(\mathbf{k}) \simeq k_x^2/2m_x + k_y^2/2m_y + k_z^2/2m_z$. The corresponding density of states at the Fermi level $N(0)$ vanishes as $N(0) \propto n^{1/3}$, for $n \rightarrow 0$, and so does the electron–phonon coupling constant $\lambda = 2N(0)g^2/\omega_{\text{ph}}$, where g is the el–ph matrix element and ω_{ph} the characteristic phonon energy scale. For this reason superconductivity in heavily doped semiconductors hardly exceeds few hundredths of mK [1]. Finally, on the experimental ground, the measured small density of carriers in the high- T_c compounds is in apparent contradiction with the sizable density of states and the large Fermi surfaces (except in MgB_2), also inferred by different experimental techniques.

We have thus to face the puzzling question: is it possible, and under which conditions, to reconcile at the same time small carrier density, finite density of states and a large Fermi surface? In this paper we are going to show that an affirmative answer to this question requires particular conditions which are fulfilled in different ways in the different families of high- T_c compounds: cuprates, fullerenes and MgB_2 . The strict constraints imposed by these requirements can account for the relative rareness of high- T_c superconductivity in solid state physics. Some qualitative consequences on the physical properties will be also discussed.

2.1 A look at conventional metals

In order to better understand the characteristic features which make cuprates, fullerenes and MgB_2 so peculiar, let us first consider the simplest case of a non-interacting metallic system, which can be used as a paradigmatic example of a conventional good metal. Moreover, these preliminary considerations will permit us to introduce in a simple but compelling way some fundamental quantities such as the Fermi energy, the carrier density, the Fermi volume, etc.

Even at the level of non-interacting systems, some care is needed in order to quantify the degree of metallic character. A first suitable parameter is given by the density of states (per spin) at the Fermi level $N(0)$, which counts the *number* of excitations available close the Fermi level. Alternatively, additional information are provided by the Fermi velocity v_F which rules the *dynamics* of the electronic excitations close at the Fermi level. From a qualitative point of view one can expect the best metallic properties for large $N(0)$ and large v_F . However these two conditions are apparently in competition with each other since one can show that $N(0)$ and v_F are inversely proportional each other. In particular:

$$N(0) = \frac{1}{V_{\text{BZ}}} \int d\mathbf{k} \delta(\varepsilon_k) = \frac{1}{V_{\text{BZ}} S_F} \int dS_k \frac{1}{|v_k|}, \quad (1)$$

where V_{BZ} is the volume of the Brillouin zone ($V_{\text{BZ}} = 8\pi^3/V_{\text{cell}} = (2\pi/a)^3$ for a cubic system) and dS_k is the infinitesimal element of the area of the Fermi surface (S_F). In the simplest case where $|v_k|$ is constant of the whole Fermi surface $|v_k| = v_F$ we obtain thus:

$$N(0) = \frac{S_F}{V_{\text{BZ}}} \frac{1}{v_F}. \quad (2)$$

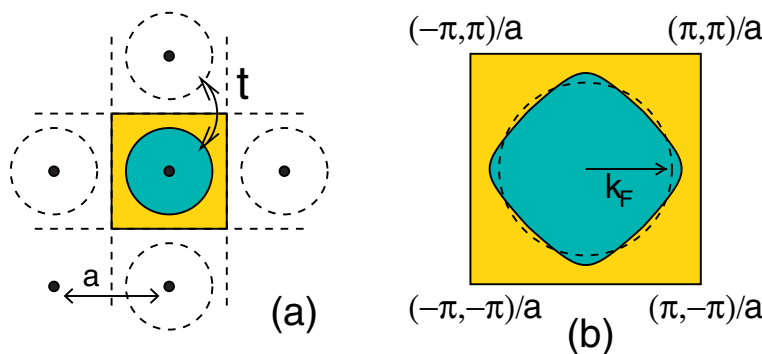


Fig. 1 (online colour at: www.pss-b.com) (a) Unit cell of a simple one-orbital cubic model. The carrier density n for unit cell is given by the filled area (twice the spin) which is roughly of the same order of V_{cell} for good metals. Hopping integral t between nearest neighbors accounts for electronic conduction and determines the band structure. (b) Brillouin zone of the cubic tight-binding model and Fermi volume (dark area). Carrier density is proportional to the Fermi volume. Dashed line: corresponding Fermi volume for an isotropic system.

We can introduce an “effective” Fermi momentum k_F by relating the *volume* of the Fermi surface to the *area* of the Fermi surface, $V_F = S_F k_F$, and to an “effective” Fermi energy $E_F = v_F k_F$, so that

$$N(0) = \frac{V_F}{V_{\text{BZ}}} \frac{1}{E_F} = \frac{nV_{\text{cell}}}{2E_F}, \quad (3)$$

where the total charge density n (including spin) is expressed as $nV_{\text{cell}} = 2V_F/V_{\text{BZ}}$. Note that the above definitions of Fermi momentum and Fermi energy apply for both electron- or hole-like conduction systems, where the charge carrier density n , Fermi momentum k_F and Fermi energy E_F indicate respectively electron or hole quantities. As we have seen above, the four parameters $N(0)$, n , V_{BZ} ($\sim V_{\text{cell}}^{-1}$) and E_F , are however not independent on each other in the simplest systems, e.g. in the case of a three-dimensional semiconductor where $E_F \propto n^{2/3}$. The most interesting situation is however when they *can* be actually considered independent; in these cases one is in principle able to find at the same time sizable density of states, small carrier density, small Fermi energy and large Fermi vectors $k_F \sim k_{\text{BZ}}$, where k_{BZ} is the maximum momentum of the Brillouin zone. As we are going to see later, these particular conditions are encountered in many high- T_c and exotic superconductors.

The simplest model of a conventional metal we can think of is a monoatomic crystal with one orbital per site, where each atom provides a certain amount x of electrons for the metallic binding. The highest metallic behavior in this simple model is attained for $x \sim 1$ while the $x \ll 1$ and $2 - x \ll 1$ limits describe respectively a n - or p -doped semiconductor (we are taking into account here the spin degree of freedom).

For the sake of simplicity we consider an electron-like conduction band where $x = x_e \lesssim 1$. This implies that the relevant quantities, such as metallic charge density n (or x), Fermi energy E_F , Fermi volume V_F , Fermi vector k_F , Fermi velocity v_F , will refer to the conduction of negative (electron) charges. The discussion will apply however as well for hole-like $x \gtrsim 1$ conduction by replacing electron with hole quantities: $x_e \rightarrow x_h = 2 - x_e$, $E_F^e \rightarrow E_F^h$, etc. In this framework the (electron) carrier density is easily obtained as $n \sim x/V_{\text{cell}}$ where V_{cell} is the volume of the unit cell (see Fig. 1a). For a cubic system $V_{\text{cell}} = a^3$ where a is the lattice constant. Typical values appropriate for this simple model are $a \sim 1 - 2 \text{ \AA}$ and $V_{\text{cell}} \sim 10^{-23} - 10^{-24} \text{ cm}^3$, so that for $x \sim 1$: $n \sim 10^{23} - 10^{24} \text{ cm}^{-3}$.

Similar estimates can be obtained from a k -based analysis in the reciprocal space (Fig. 1b), which permits also to relate the carrier density n to directly measurable quantities as the Fermi energy E_F , the Fermi volume V_F or the Fermi vector k_F . We can estimate the total number of electron charges x for unit cell as $x = 2V_F/V_{\text{BZ}}$, where V_F is the Fermi volume and the factor 2 takes into account the spin degeneracy.

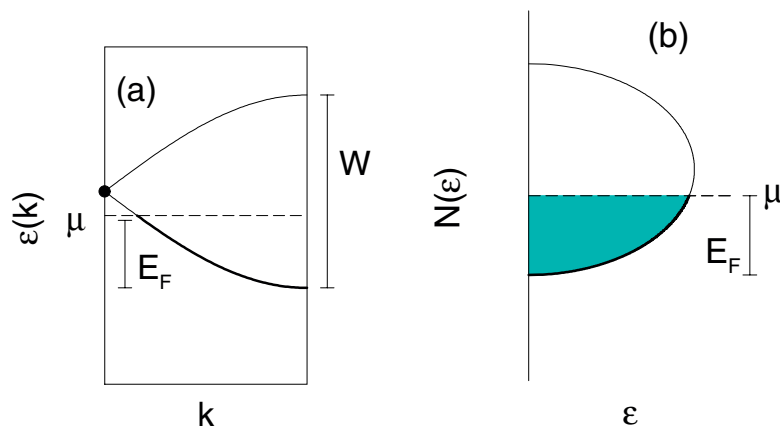


Fig. 2 (online colour at: www.pss-b.com) (a) Schematic picture of the electron dispersion for the monoatomic model. The bandwidth W scales as $W = 2dt$ where d is the physical dimension and t the hopping integral. The electron carrier density is proportional to the number of k states (thick line) below the chemical potential μ . (b) Schematic DOS for a three-dimensional system. In this case the carrier density is proportional to the *integral* of the density of states up to the chemical potential.

The best metallic behavior is encountered at the half-filling ($x=1$) where the Fermi surface is the largest, while the vanishing electron-like or hole-like Fermi volumes correspond respectively to n - and p -doped semiconducting systems. From the above estimates of the electron density, using $V_F = S_F k_F$ and an isotropic expression for a three-dimensional Fermi surface $S_F = 4\pi k_F^2$, we obtain for $x=1$: $k_F \sim 1 - 2 \text{ \AA}^{-1}$.

It should be noted that the two pictures outlined above to estimate the charge density, both in the direct and reciprocal spaces, are based on only *length scales*. Interesting implications come however relating the amount of charge carriers to the relevant *energetic scales* of the system. A first natural energy scale, in the simple tight-binding model considered here, is set by the hopping integral t between nearest neighbor orbitals, which also determines the electronic bandwidth W (Fig. 2a). A second energy quantity is provided by the electronic Fermi energy E_F , conventionally determined as $E_F = \mu - E_{\text{edge}}$ where μ is the chemical potential and E_{edge} the nearest band-edge to μ (bottom for electron conduction, top for holes). At zero temperature $T = 0$ the electron density x for unit cell reads:

$$x = \frac{2}{V_{\text{BZ}}} \int dk \theta[\mu - \varepsilon_k], \quad (4)$$

where ε_k is the electronic dispersion with bandwidth W . Moreover Eq. (4) can be expressed in the form:

$$x = 2 \int d\varepsilon N(\varepsilon) \theta[\mu - \varepsilon_k], \quad (5)$$

where we have introduced the electronic density of states (DOS) per spin $N(\varepsilon)$. Simple sum rules show that $N(\varepsilon)$ scales as $N(\varepsilon) \sim 1/t$. In particular, for an equally distributed density of states (constant DOS) we have $N(\varepsilon) = 1/W$ for $\varepsilon \in [-W/2, W/2]$. The value $1/W$ can be also regarded as the mean value of the electronic density of states averaged over the whole Brillouin zone. From Eq. (5) we get:

$$E_F \approx x \frac{W}{2}. \quad (6)$$

Equation (6) is just the same as Eq. (3) confirming the equivalency between the two approaches. Optimal metallic properties, close to half-filling, are thus obtained for $E_F \approx W/2$, while $E_F^c = E_F \ll W/2$ and $E_F^h = W - E_F \ll W/2$ correspond once more to the limits of n - and p -doped semiconductors (Fig. 2).

In order to provide a numerical estimate of all the quantities related to the energetics of the conduction band, we need now to specify the energy scale of the conduction bandwidth W , or equivalently of the hopping term t . On physical grounds, these parameters depend in an implicit way on the lattice constant a , which determines the atomic orbital overlapping, and on the nature of the atomic orbitals (s -, p -, d -, f -bands). Typical examples of good metals are constituted by close packed atoms with lattice spacing a of the order $\sim 1 - 2 \text{ \AA}$ and bands with s or p character. In this situation $t \sim 0.5 - 1 \text{ eV}$ and $W \sim 5 - 10 \text{ eV}$, so that $E_F \sim 2 - 5 \text{ eV}$, $v_F \sim 10^7 \text{ cm/s}$.

2.2 Playing with parameters in conventional metals

In the previous section we have summarized, with the help of a simple model, the main properties of conventional metals, which apply qualitatively to the low- T_c superconductors. Among other properties: a sizable carrier density $n \sim 10^{23} - 10^{24} \text{ cm}^{-3}$, large Brillouin volumes $V_{\text{BZ}} \sim 10^1 - 10^2 \text{ \AA}^{-3}$, a large magnitude of carrier density *with respect to* the Brillouin volume $x = 2V_F/V_{\text{BZ}} \sim 1$, large Fermi momenta in comparison with the Brillouin momentum $k_F/k_{\text{BZ}} \sim 1$, large Fermi energies $E_F \sim 2 - 5 \text{ eV}$, relatively small densities of states $N(0) \sim 0.1 - 0.3 \text{ states}/(\text{spin} \cdot \text{eV})$. It should be noted however that this scenario was drawn assuming a finite amount $x \sim 1$ of charge carriers per unit cell in the simple model above discussed and assuming a closely packed structure. Low carrier density features can arise in this framework

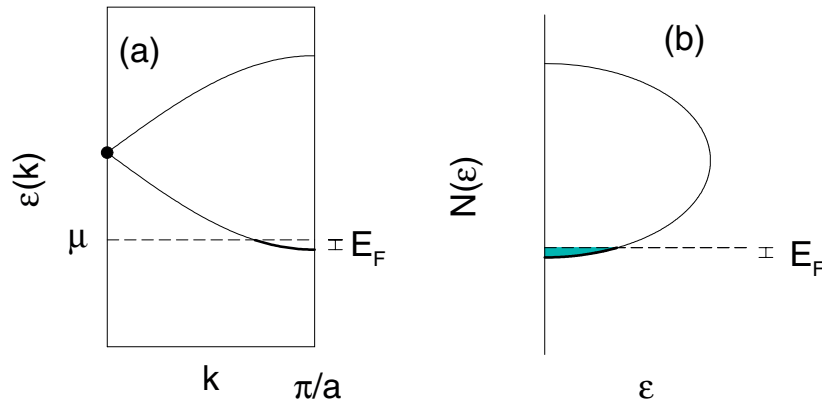


Fig. 3 (online colour at: www.pss-b.com) Schematic picture of a low carrier density with a small amount of charge per unit cell. (a) electron filling of the band structure; (b) band filling of the density of states.

either relaxing one of these two conditions (namely $x \ll 1$ or highly spaced structures), or by more sophisticated models which take into account some new physics. As we are going to see, the first situation applies to conventional low carrier density systems (such as doped semiconductors, for instance), the latter one to cuprates and fullerenes. We shall first discuss qualitatively the case of doped semiconductors, which will be instructive to underline the novel traits of fullerenes and cuprates.

Low carrier density features are obtained in the most straightforward way in the one-orbital model when the charge amount for unit cell available for metallic binding is quite small $x \ll 1$ (Fig. 3). In the extreme limit $x \rightarrow 0$ we obtain a band insulator where all the Fermi parameters go to zero: $S_F, v_F, V_F, E_F, k_F \rightarrow 0$ and no charge carrier can travel. In metals with a small amount of free charge per orbital or in doped semiconductors where additional charge is supplied by external doping centers we can still establish a metallic behavior, although with extremely small Fermi parameters $V_F \ll V_{BZ}, k_F \ll k_{BZ}, E_F \ll W$. This situation however appears unfavorable for superconductivity for different reasons. On one hand the reduced metallic character has to compete with other local mechanisms (exciton, polaron, Anderson's localization, ...) which tend to destroy itinerant Bloch-like properties. On the other hand, as already mentioned above, for three-dimensional systems the density of states close to the band edge scales as $N(0) \propto n^{1/3} \propto \sqrt{E_F}$ (Fig. 3). El-ph metallic and superconducting properties, which rely on the quasiparticle concept and are ruled by the el-ph coupling constant $\lambda = 2N(0)g^2/\omega_{ph}$, are thus correspondingly reduced whereas el-ph polaron features, related to the parameter $\alpha^2 = (g/\omega_{ph})^2$, still survive.

An alternative (theoretical) way to achieve low carrier densities within the framework of the simple model with one orbital per unit cell is assuming unrealistically large lattice parameters. In this case the low charge density $n = x/V_{cell}$ is related more to the large volume of the unit cell V_{cell} than to the small value of x . This situation has some interesting consequences. First, Fermi-like parameters such as V_F, k_F, E_F , are not negligible in comparison to the corresponding Brillouin quantities V_{BZ}, k_{BZ}, W . This assures a quite reasonable metallic character even in the presence of small carrier density. Secondly, this implies small values of the hopping integral t between nearest neighbor orbitals, leading to narrow bandwidths and small Fermi energies. Finally, small values of Fermi energy E_F imply strong electronic correlation effects when $x \approx 1$ and when E_F is comparable with the local Hubbard repulsion U . The remarkable resemblance between this scenario and the theoretical and experimental one observed in cuprates and fullerenes could suggest that it applies in a straightforward way to these materials. However there are two main drawbacks which make it not suitable to be applied as it is to the high- T_c superconductors. The first one is the chemical binding which tends to favour the close-packed structures with compact unit cells. Later we shall see how this issue is addressed in fullerene compounds. The second objection is that the electron-phonon matrix elements g in this model are mainly related to the derivative of the hopping

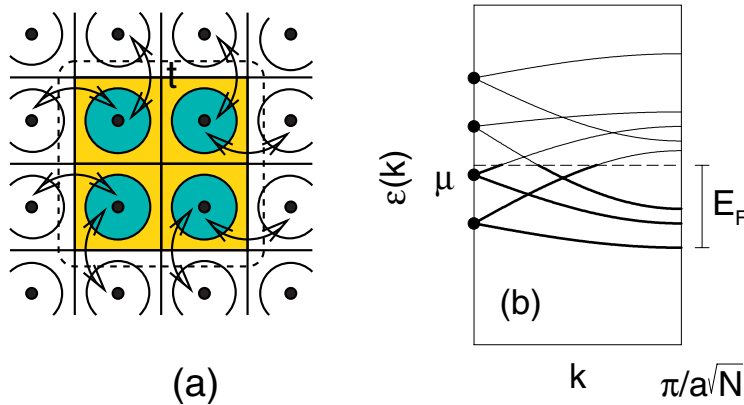


Fig. 4 (online colour at: www.pss-b.com) (a) Artificial construction of molecular crystal in terms of N unit supercell; (b) Schematic band structure corresponding to panel (a): filled dots represent the discrete molecular energy levels which gain dispersion from the inter-molecular hybridization terms.

integrals with respect to the atomic displacement u from the perfect periodic structure, $g \propto t' = dt/du$. Large lattice spacings imply thus small values of t' as well as of t , and the total electron–phonon coupling is thus expected to be significantly reduced.

As we are going to discuss in the next section, low carrier densities in the presence of good metallic character are attained in fullerenes because of their molecular crystal structure, where the unit block is represented by a large molecule composed of several atoms. Before addressing the specific characteristics which make the fullerenes so interesting, let us now consider as an instructive example the simple model above discussed with just one orbital in close packed unit cells. The same system can be artificially described in terms of a molecular crystal by introducing a coarse-grained supercell made by N unit cells (Fig. 4a). Of course, since it is just a different representation of the same thing, we have to obtain the same results. The identity between the two representations is trivial in real space where the charge density in the supercell system is simply given by $n = Nx/[NV_{\text{cell}}] = x/V_{\text{cell}}$. The connection is however highly instructive when regarded in terms of band structure. Let us consider first the N -supercell alone where the inter-supercell hybridization terms are neglected. Since the internal electronic energy scale is set by t , the molecular spectrum is given by a discrete set of N energy levels distributed in a energy window $\approx W \propto t$ (Fig. 4b). Each of these molecular energy levels will gain a finite dispersion of the order of t from the hybridization between neighbor supercells once the supercell molecule is plugged in the truly periodic lattice structure. The total band structure, in the reduced Brillouin zone relative to the N -supercell, will be thus composed by a set of N highly overlapping bands. Each of these bands will account, on average, for a carrier density $n = 2\tilde{V}_F$, where $\tilde{V}_F = V_F/N$. Some considerations about this simple model of molecular crystal can be advanced. First, it is clear that it is not undermined by stability problems since it is just a different view of a monoatomic simple metal. Secondly, electronic scattering with “inter-molecular” phonons (lattice vibrations with wave-length larger than the size of the supercell) arises from the same lattice modulation as the hopping term t which rules electronic scattering with “intra-molecular” phonons (lattice vibrations with wave-length smaller than the size of the supercell); both of them are expected to contribute significantly to the total el–ph coupling. However, we must also note that this simple-minded supercell molecular crystal does *not* describe a low carrier density system: a N -supercell molecule contains a bigger amount of charge in a larger volume, giving a charge density which is just the same as that of a monoatomic metal. In a similar way, the strong hybridization between neighbor molecules leads to wide band electronic dispersions and to a large Fermi energy $E_F \sim W/2$. As we are going to see, the link between carrier density and Fermi energy holds true even in more complex materials, as fullerenes and cuprates, where the *small* carrier density character is associated to *small* Fermi energies.

3 Complex models for unconventional superconductors

In the previous section we have reviewed some simple considerations which permit to relate, in conventional metals, the amount of charge carriers to the superconducting pairing and to other physical properties in both the real and reciprocal space. We have paid particular attention in relating the carrier density n to energy scales such as the Fermi energy E_F , the electron bandwidth W , the orbital hybridization t etc. In the same context we have also described conventional low carrier density systems (such as doped semiconductors) in terms of extreme values of physical parameters (the lattice spacing a , the amount of charge density for unit cell x , ...). Although these simple models are quite far from the experimental characteristics of the high- T_c superconductors, their comparison with more complex models permits to highlight some of the peculiar unconventional features of the high- T_c materials.

As we are going to see, fullerenes, cuprates and also diboride alloys follow different routes to reconcile low carrier density, sizable density of states and electron–phonon coupling, and small Fermi energy.

3.1 Fullerenes and molecular crystals

One of the most interesting families of materials which fulfill these characteristics is the family of molecular crystals, where the elementary unit of the periodic structure is made by a macromolecule. Typical bonds between molecules are of the Van der Waals type.

In the following we shall focus on the C_{60} compounds, which are the most representative case and which show the highest superconducting critical temperatures [50]. In this case the elementary unit is given by a “soccer” ball of 60 carbon atoms with a radius $r \sim 7 \text{ \AA}$. Pristine C_{60} is an insulator with a fcc structure and cubic lattice parameter $a \approx 14 \text{ \AA}$. In the superconducting family A_3C_{60} , free conduction carriers are typically provided by doping with alkali atoms which completely ionize and which slightly enhance the lattice constant ($a_{A_3C_{60}} \sim 14.4 - 14.5 \text{ \AA}$). Trivial calculations estimate thus in a straightforward way a carrier density $n \sim 4 \times 10^{21} \text{ cm}^{-3}$, two orders of magnitude less than the previous estimates for conventional metals. One could be tempted to attribute this remarkable reduction of charge density to the large portions of empty space *between* and *within* the C_{60} molecules, yielding a fcc cell volume $V_{\text{cell}} \sim 3 \times 10^{-21} \text{ cm}^3$. However, if we estimate the total equivalent volume which would be needed to accommodate, in the compact diamond structure, the total number of 240 carbon atoms contained in the fcc cell we would get $V_{\text{diam}}^{\text{equiv}} \sim 1.35 \times 10^{-21} \text{ cm}^3$, which accounts just for a factor 2 of reduction. As a matter of fact, the effective reason of such a small carrier density is related more to the number of molecular orbitals involved in the conduction band than to the size of the unit cell. Once more, energetic considerations can help to gain a deeper insight about this concept.

A useful insight comes from comparing the C_{60} molecule with the previous example of a N -atom supercell. As far as we deal with a single molecule, the two objects look quite similar. Density functional analyses show that the molecular orbitals with energies close to the chemical potential are mainly determined by the p_z carbon orbitals [51], so that the C_{60} can be effectively regarded as a 60-atom molecule with just one orbital per atom. Group theory helps to rearrange the Hilbert space of 60 atomic orbitals in terms of a set of molecular levels. The energy spacing between molecular level is determined by the large carbon–carbon binding energy scale t_{C-C} , which leads, for example, to a gap $\sim 2.0 \text{ eV}$ between the h_u highest occupied molecular orbitals (HOMO) and the l_{lu} lowest unoccupied ones (LUMO) [51].

We then consider the C_{60} molecule as the basic cell for the solid fcc alkali-doped A_3C_{60} structure. Crucial differences between the “supercell” model and molecular crystals appear when we compare the inter-molecular hybridization energy scale $t_{C_{60}-C_{60}}$ with the intra-molecular one t_{C-C} (see Fig. 5). Roughly speaking, the intra-molecular scale t_{C-C} determines the energy spacing between molecular levels, while the weak overlap between neighboring C_{60} molecular orbitals, $t_{C_{60}-C_{60}}$, gives rise to the electron band dispersion. The energy scale of the latter processes are usually much smaller than the gap between different molecular levels, so that the resulting band structure is described by a set of narrow bands as depicted in Fig. 6b. For the case of the t_{lu} bands in the alkali-doped A_3C_{60} compounds, tight-binding calcu-

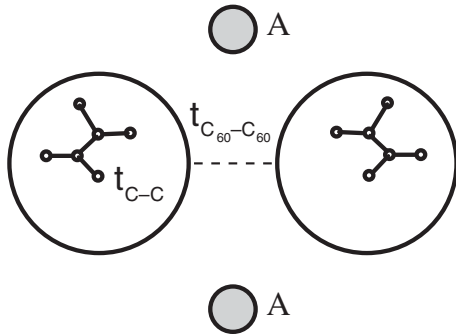


Fig. 5 Comparison of energy scales in C_{60} compounds. Intra-molecular energy are ruled by the strong carbon-carbon bond t_{C-C} , while the weak overlap between molecular orbitals of different buckyballs leads to a much smaller energy scale $t_{C_{60}-C_{60}}$.

lations estimate the nearest-neighbor hopping terms $t_{C_{60}-C_{60}}$ to be of the order of 10–40 meV, giving rise to half-bandwidths of the order of $W/2 \sim 250-300$ meV [52], to be compared with the ~ 2 eV gap between t_{1u} and h_u molecular levels [50].

This scenario has interesting consequences about: *i*) the charge carrier density. Only three of the 60 bands arising from the 60 molecular orbitals cross the Fermi level and they can be considered as conduction bands. Other bands lie so far below the Fermi level that they can be regarded in good approximation as valence bands. This is quite different from what happens in the supercell model where, since the bandwidths are of the same order of the molecular level spacing, a large part of the molecular bands contribute to the metallic conduction (Fig. 6a). The ratio 3/60 ($\sim 1/20$) between the conduction bands and the total available bands gives thus a rough estimate of the charge carrier density reduction in A_3C_{60} compounds with respect to conventional metals where each unit cell orbital contributes equally to the metallic character. *ii*) the relation between charge carrier density and energy scales. In particular the strict connection between small carrier density and small Fermi energy is evident from the above discussion and it is related to the marked separation between the inter- and intra-molecular electronic energy scales $t_{inter} \ll t_{intra}$. We note however that the lower lying or higher lying bands could provide in principle additional effective metallic charges for what concerns transport and superconducting properties when the phonon energy ω_{ph} is large enough to involve them in the electron–phonon scattering. While this is

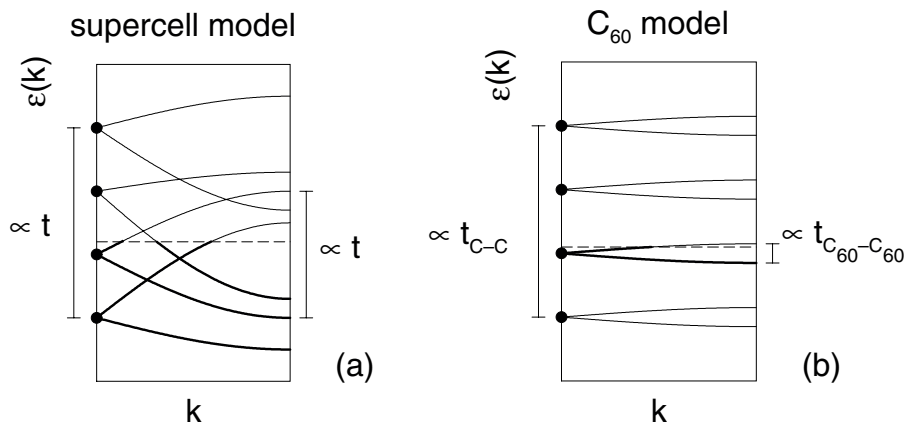


Fig. 6 Comparison between the schematic band structure of the “supercell” model and of molecular (C_{60} compounds) crystals. Filled dots mark the molecular spectrum. In the supercell model the energy scale ruling the spreading of the molecular levels is the same which gives rise to the band dispersion (panel a). On the other hand in fullerenes band dispersion is determined by the inter-molecular hopping terms $t_{C_{60}-C_{60}}$ which are much weaker than the electronic intra-molecular energy scale t_{C-C} . Metallic charges are determined by the number of the filled k states (thick lines) of the conduction bands.

Table 1 Schematic phase diagram for electronic correlation. Electronic correlation effects are relevant when *both* U is comparable with the electronic kinetic energy scale E_F and the systems are close to half-filling $x \sim 1$. The case $x \sim 1$ and $U \ll E_F$ corresponds to conventional metals while $x \ll 1$ and $U \sim E_F$ to doped semiconductors.

	presence of electronic correlation effects	
	large E_F systems $U \ll E_F$	small E_F systems $U \sim E_F$
low band filling ($x \ll 1$)	NO	NO
sizable band filling ($x \sim 1$)	NO	YES

not the case in C_{60} and other molecular crystal compounds, some of these effects could be present in metallic and semiconducting carbon nanotubes where the energy gap between lower (upper) subbands and Fermi level can be of the same order of the highest phonon frequencies ~ 0.2 eV. *iii*) the relevance of the electron–phonon interaction. The energy separation between inter- and intra-molecular processes is reflected also in the magnitude of the corresponding electron–phonon matrix elements that, as we briefly discussed above, are generically proportional to the derivative with respect the lattice displacements, $g \propto dt/du$. Consequently the small carrier density character and small Fermi energies in fullerenes and molecular crystals are intrinsically linked with a weak inter-molecular electron–phonon scattering, but they are perfectly compatible with a significant intra-molecular electron–phonon coupling, which is related to the strong carbon–carbon binding ruled by t_{C-C} , while the Fermi energy is ruled by $t_{C_{60}-C_{60}}$ [53].

An additional interesting feature of this scenario is the crucial role played by the onsite electronic correlation. This is quite remarkable since onsite electronic correlation and a low carrier density character are usually considered mutually exclusive issues. Simple arguments to understand this statement come from considering the paradigmatic Hubbard model,

$$H = \sum_{k,\sigma} \varepsilon_{k\sigma} c_{k\sigma}^\dagger c_{k\sigma} + U \sum_i n_{i\uparrow} n_{i\downarrow}, \quad (7)$$

which contains the minimal ingredients to describe correlated systems. Electronic correlation arises from the competition between the kinetic term, which favors Bloch-like propagation, and the second (Hubbard) term which suppresses onsite double occupancy and tends to localize the electronic states. The degree of electronic correlation is then ruled by essentially only two parameters: the electronic filling x and the magnitude of the Hubbard term with respect to the electronic kinetic energy U/E_F . The strongest correlation effects appear when $U/E_F \sim 1$ and $x \sim 1$ (half-filling), eventually leading to a Mott–Hubbard metal–insulator transition in the extreme case $x = 1$ and U/E_F greater than a critical value $U/E_F \geq U_c/E_F$. On the other hand electronic correlation effects are expected to be negligible both in conventional good metals with large Fermi energies, where $x \sim 1$ but $U/E_F \ll 1$, as well as in conventional low carrier density systems (doped semiconductors) where $U/E_F \sim 1$ but $x \ll 1$ (see Table 1).

We can note that the very features which characterize the nonadiabatic metals with low carrier density, namely the small Fermi energies *in the presence* of large Fermi surfaces and a sizable filling of the Brillouin zone, make these materials ideal candidates for strong electronic correlation effects. In the case of the fullerene compounds, for instance, band structure calculations in $A_3 C_{60}$ predict three roughly half-filled bands with a Hubbard repulsion $U \sim 1–1.2$ eV, which has to be compared with $E_F \sim 0.25–0.3$ eV [50], pointing out remarkable strong correlation effects probably close to a Mott–Hubbard metal–insulator transition.

The precise role of the electronic correlation on the main physical properties of fullerenes and its interplay with the electron–phonon interaction in the nonadiabatic regime has been widely investigated in the past and it is still an open issue. A more detailed discussion of the consequences of the electronic correlation in C_{60} compounds is out of the purposes of this paper [50]. What we would like to underline

here is that the very conditions which make the fullerenes reconcile low carrier density, small Fermi energy, large Fermi surfaces, give rise to relevant correlation effects. Electronic correlation appears thus as an unavoidable product. As we are going to see, electronic correlation will play a fundamental role even in a different class of low carrier density materials, the cuprates, although in a somewhat different way.

3.2 Cuprates and correlation effects

Copper oxides are characterized by a strong anisotropy of the electronic and superconducting properties, where coherent metallic conduction and the superconducting ordering are mainly confined into the Cu–O layers [54]. For these properties cuprates can be thus considered to a large extent as bidimensional, so it is useful to express the “cubic” charge carrier density n in terms of the in-plane charge density $n_{2D} = nd$ [23, 24], where d is the out-of-plane lattice parameter which can be quite different in the different subfamilies of cuprates (LSCO, BiSSCO, YBCO, ...). For the sake of shortness, in the following we shall call n_{2D} charge carrier density, by understanding it is referred to the planar charge density. The unit cell in the Cu–O plane contains simply one copper and two oxygen atoms, with a in-plane lattice constant $a_{\text{Cu–Cu}} \sim 3.8–4.0 \text{ \AA}$ [54]. First principle band structure calculations are reproduced at a very good approximation by a so-called three-band tight-binding model [55–57]. In the parent undoped compounds each carbon and oxygen atom contributes respectively one free electron and one orbital (per spin) ($d_{x^2-y^2}$ for Cu, p_x and p_y for O) to the total Hilbert space. The low energy part of the band structure can be further simplified by introducing the Zhang–Rice singlet [58]. The electronic dispersion is thus expressed in terms of a one-band tight-binding model, with one free electron and one spin double-degenerate orbital (the Zhang–Rice singlet) for each site of a square lattice. According to this scenario, undoped copper oxides would be expected to be described in terms of common metals with roughly half-filled bands $x = 1$ and significant charge densities. Further charges, usually holes, can be introduced into the copper-oxygen plane by different stoichiometric substitutions of the out-of-plane atoms [54]. The total charge carrier density is thus expected to scale as $x \sim 1 - \delta$, where δ is the density of holes for unit cell.

At first sight the cuprates might appear as a good example of conventional metals. In the spirit outlined in Sec. 2.1 and Figs. 1, 2, we could estimate for instance a charge carrier density $n_{2D} = x/V_{\text{cell}}^{2D} = 10^{14} - 10^{15} \text{ cm}^{-2}$. This value is not far from what is found by penetration depth measurements in overdoped LSCO, BiSSCO and YBCO, assuming a band-like electron mass $m = 5m_e$ [23, 24]. However, the experimental dependence of n_{2D} on the hole doping strongly questions a simple description of cuprates in terms of conventional metals, showing an almost linear decrease of $n_{2D}(\delta)$ as δ decreases $\delta \rightarrow 0$. This trend is in contrast with the common metal picture where the charge density $n \propto 1 - \delta$ is expected to be roughly independent of δ as $\delta \rightarrow 0$. Resistivity measurements find a similar linear scaling of the metallic behavior with the hole doping δ [59]. The most extreme case is the half-filling one $\delta = 0$, $x = 1$, where cuprates are found to be insulators whereas the above conventional picture would predict a half-filled band metal.

Once again, to gain a deeper insight in these materials and to understand these discrepancies, we need to resort to energetical considerations. One of the main features which differentiates the cuprates from conventional metals is the high degree of electronic correlation. Like other transition compounds with strong d or f character, the electronic structure in cuprates is indeed characterized by narrow bands and by a strong onsite Coulomb repulsion due to the reduced orbital penetration of the $d_{x^2-y^2}$ states [60]. Typical energy scales are for instance a Hubbard term $U \sim 5 \text{ eV}$ and a kinetic Fermi energy $E_F \sim 0.3 - 0.4 \text{ eV}$ [54, 55, 61]. In this situation, as briefly discussed in the previous section, electronic correlation effects play a crucial role on many physical properties of these materials, especially close to half-filling where a Mott–Hubbard metal–insulator transition is expected. This qualitative picture is confirmed by the experimental phase diagrams of the cuprates, which show an anti-ferromagnetic phase at half-filling established on the top of a Mott–Hubbard insulating state. Metallic properties evolve in a continuous way upon doping which provides further positive (or negative) charges respectively in hole or electron-doped cuprates.

In this contribution we do not attempt to provide a comprehensive overview of the many unconventional characteristics of strongly correlated systems, but we would like rather to focus in the most intui-

tive terms on the strict link between charge carrier density, Fermi energies E_F , Fermi volume V_F , density of states etc ..., even in this class of materials. Note that to this aim only one-particle properties, which can be directly related to the knowledge of the one-particle Green's function $G(\mathbf{k}, \omega)$, are involved. A crucial point in strongly correlated systems is to distinguish between a *coherent* part of the one-particle Green's function $G(\mathbf{k}, \omega)$ and an *incoherent* one [62]:

$$G(\mathbf{k}, \omega) = G_{\text{coh}}(\mathbf{k}, \omega) + G_{\text{inc}}(\mathbf{k}, \omega), \quad (8)$$

where $G_{\text{coh}}(\mathbf{k}, \omega)$ describes quasi-particle Bloch-like electrons for which \mathbf{k} is a good quantum number, and $G_{\text{inc}}(\mathbf{k}, \omega)$ corresponds to the incoherent background with a weak dependence on the electronic momentum. Conduction properties, as metallic charge density, Fermi volume, Fermi energy etc., are mainly associated with $G_{\text{coh}}(\mathbf{k}, \omega)$.

A qualitative instructive picture for $G_{\text{coh}}(\mathbf{k}, \omega)$ is provided by the Gutzwiller solution [63] which approximates the coherent metallic part of the Green's function with that of an effective model of non-interacting particles with reduced spectral weight and reduced bandwidth:

$$G_{\text{coh}}(\mathbf{k}, \omega) = \frac{Z}{\omega - Z\varepsilon_{\mathbf{k}} + \mu}. \quad (9)$$

On a physical ground, the quasi-particle spectral weight Z is expected to depend on the band filling and on the Hubbard repulsion U . For a common metal we have $Z = 1$, while the Mott–Hubbard metal–insulator transition corresponds to $Z \rightarrow 0$, which occurs at half-filling and $U \geq U_c$. Note that, while Eq. (9) implies a renormalization of the electronic kinetic energy $E_F \rightarrow ZE_F$ and of the quasi-particle weight $Z < 1$, which is directly associated with the effective amount of charge carriers, no significant effect is predicted in the *momentum* space, i.e. the volume of the Fermi surface is not affected by correlation effects and Luttinger's theorem is preserved.

Equation (9) encloses in a simple approximate way the fundamental differences between a band insulator and a Mott–Hubbard metal–insulator transition. In qualitative terms, while in conventional metals insulating properties are related to the vanishing of the Fermi volume, which is proportional to the total charge, with respect to the total Brillouin volume, the Mott–Hubbard metal–insulator transition is described in terms of transfer of spectral weight from the coherent to the incoherent part (which is not associated with metallic properties), with a corresponding vanishing of the metallic character for given amount of charge. This has important consequences on the relation between metallic charge carrier density, the electron density of states, Fermi energy and the Fermi volume.

Simple qualitative relations between these physical quantities were derived in Sec. 2.1 in the case of conventional metals. We can now generalize them in an appropriate way in correlated systems with the help of Eq. (9). To this aim it is useful to distinguish between quasi-particle (metallic) quantities, related to the coherent part of the Green's function, and the quantities which are related to the incoherent localized background of $G_{\text{coh}}(\mathbf{k}, \omega)$. In particular, generalizing Eq. (4), the total amount of *metallic* charge for unit cell in the correlated system can be expressed as:

$$\bar{x} = -\frac{2}{V_{\text{BZ}}} \int d\mathbf{k} \int \frac{d\omega}{\pi} f(\omega) \text{Im} G_{\text{coh}}^{\text{R}}(\mathbf{k}, \omega) = \frac{2}{V_{\text{BZ}}} Z \int d\mathbf{k} \theta[\mu - Z\varepsilon_{\mathbf{k}}], \quad (10)$$

where $f(\omega)$ is the Fermi function and G^{R} denotes the retarded part of the Green's function. By introducing the density of states of the uncorrelated system $(1/V_{\text{BZ}}) \int d\mathbf{k} \rightarrow \int d\varepsilon N(\varepsilon)$, we obtain thus, for a simple constant DOS model ($N(\varepsilon) = 1/W$),

$$\bar{x} = \frac{2}{W} (ZE_F), \quad (11)$$

which shows in the clearest way the direct link between the reduction of Fermi energy and reduction of the charge carrier density $n \sim \bar{x}/V_{\text{cell}}$ (V_{cell} is of course not affected by correlation effects).

The density of states at the Fermi level of the correlated system, $\bar{N}(0)$, can be also evaluated in similar way as:

$$\bar{N}(0) = -\frac{1}{\pi V_{\text{BZ}}} \int d\mathbf{k} \operatorname{Im} G_{\text{coh}}^{\text{R}}(\mathbf{k}, \omega = 0) = \frac{Z}{\pi V_{\text{BZ}}} \int d\mathbf{k} \delta(Z\varepsilon_{\mathbf{k}}) = N(0), \quad (12)$$

which shows that correlation effects do *not* renormalize the effective density of states. This is an important result since it points out that the electronic correlation can represent a tuning parameter which permits to achieve low carrier density regime and small Fermi energies in the presence of a finite density of states, and hence of a sizable electron–phonon coupling. An additional interesting quantity which is directly related to the metallic properties is the Drude conductivity σ_{D} , which in the bubble approximation can be evaluated as [64]:

$$\sigma_{\text{D}} \propto \frac{1}{V_{\text{BZ}}} \int d\mathbf{k} [\mathbf{v}_{\mathbf{k}} \cdot \mathbf{v}_{\mathbf{k}}] \int \frac{d\omega}{2\pi} f'(\omega) [\operatorname{Im} G_{\text{coh}}^{\text{R}}(\mathbf{k}, \omega)]. \quad (13)$$

Using Eq. (9) we obtain thus, for the $T = 0$ Drude conductivity $\bar{\sigma}_{\text{D}}$ of the correlated system,

$$\bar{\sigma}_{\text{D}} = Z\sigma_{\text{D}}^0, \quad (14)$$

where σ_{D}^0 is the Drude conductivity of the uncorrelated one.

The above scenario can be now applied in the specific case of the copper oxides where, as briefly mentioned above, the relevant role of the electronic correlation is implicitly confirmed by the observation of a Mott–Hubbard insulating phase close to half-filling, indicating $U > U_{\text{c}}$. For practical purposes U can be assumed to be larger than any other energy scale in the system, namely $U \rightarrow \infty$. In this situation, the only tunable parameter ruling the degree of the electronic correlation is represented by the band filling, which can be varied from the experimental point of view by chemical doping. Using the simple Gutzwiller solution, the quasi-particle spectral weight Z can be thus expressed as function of the chemical doping δ ($\delta = 1 - x$ for hole-doped cuprates) by the simple relation $Z_{\text{Gutz}}(\delta) \propto \delta$ for $\delta \rightarrow 0$ [63], estimating a reduction of the spectral weight and of the Fermi energy scales by a factor 3–6 in the relevant doping range for cuprates $\delta \sim 0.15 - 0.3$. Recent experimental data extracted by angle-resolved photoemission spectroscopy suggest a similar range of values [65]. The linear relation between the Drude conductivity and the quasi-particle spectral weight, Eq. (14), can also account for the unconventional scaling of the resistivity with the hole doping observed in Ref. [59]. Electron correlation effects are probably responsible also for the lack of resistivity saturation in cuprates and fullerenes. Proper estimates of the mean-free path, and hence of the resistivity saturation limit ρ_{sat} , should be indeed take into account the reduction of the quasi-particle spectral weight. This would predict an increase of the resistivity limit with respect to an uncorrelated system, $\bar{\rho}_{\text{sat}} \sim \rho_{\text{sat}}/Z$, beyond the experimental range of temperature.

Note that the reduction of the metallic charge density can be even smaller in the interesting case when two different parameters, Z_{qp} and Z_{w} , respectively rule the reduction of the quasi-particle spectral weight and of the electronic band dispersion. This situation is encountered in more sophisticated models, as the t – J one, where the antiferromagnetic exchange provides an additional channel of propagation for the positive hole charges. In the $U = \infty$ limit the Gutzwiller-slave-boson mean-field solution gives for instance $Z_{\text{qp}} \approx \delta$ and $Z_{\text{w}} \approx \delta + \alpha J$, where the constant α is of the order of $\alpha \sim 0.25$. One can easily check in this case that the relations (11–13) are respectively replaced by $\bar{x} = (2/W)(Z_{\text{qp}}E_{\text{F}})$, $\bar{N}(0) = (Z_{\text{qp}}/Z_{\text{w}})N(0)$ and $\bar{\sigma}_{\text{D}} = (Z_{\text{qp}}^2/Z_{\text{w}})\sigma_{\text{D}}^0$.

3.3 MgB₂ and diboride alloys

In the previous section we have illustrated along qualitative lines the peculiar structural and electronic properties of fullerenes and copper oxides which make these materials to differ from conventional low carrier density compounds. We have seen that, although due to different reasons, both fullerenes and cuprates reconcile low charge carrier density with metallic properties like a large Fermi volume, finite

density of states, etc. ... Particular care has been paid to analyze the relation between these quantities and energy scales. Along this perspective we have underlined the strict connection between low carrier density and small Fermi energy, which make these compounds ideal candidates for nonadiabatic effects.

In this section we would like to conclude this overview by briefly analyzing the case of the magnesium diboride MgB_2 . Unlike fullerenes and cuprates, which have a well defined character for what concerns the electronic band structure (three-dimensional for C_{60} compounds, bidimensional for cuprates), first principle calculations predict in MgB_2 two qualitatively different kind of bands at the Fermi level, namely two σ bands with a strong bidimensional character mainly related to the in-plane hybridization of the boron p_x and p_y orbitals, and two π bands with three-dimensional character involving Mg and boron p_z orbitals [66, 67]. The Fermi level crosses the σ bands very near to their top band edge, yielding two small hole pockets close the Γ point. Band structure calculations find $x^\sigma \sim 0.067$ per unit cell and per band [67], which gives a mean planar charge density for each σ band $n_{2D}^\sigma \sim 8 \times 10^{13} \text{ cm}^{-2}$. This value could be compared with the one estimated from in-plane penetration depth measurements [68] which give $n_{2D}^\sigma \sim 2 \times 10^{13} \text{ cm}^{-2}$, using a mean value for the σ band-like masses $m/m_e \approx 0.365$. Although the value of n_{2D}^σ extracted by penetration depth data has to be considered purely indicative since it involves finite contributions from the three-dimensional π states, the qualitative agreement points out that the low charge carrier density of the σ bands can be indeed understood in terms of weakly filled bands, in the context described in Sec. 2.2 and Fig. 3. Coherently with this picture, the small carrier density is associated with a small Fermi energy of the hole charges in the σ bands, $E_F^\sigma \approx 0.4 - 0.6 \text{ eV}$, which can be compared with the a bandwidth $W^\sigma \approx 6 - 8 \text{ eV}$ [66, 67].

In Sec. 2.2 we have mentioned the case of weakly filled systems as the most trivial way to reconcile low carrier density and small Fermi energy, leading to the onset of nonadiabatic electron–phonon effects. This situation has been however claimed to be unfavorable to a large superconducting pairing because of the corresponding small density of states $N(0)$ in three-dimensional systems $N(0) \propto n^{1/3} \propto \sqrt{E_F}$. We are now faced now with two basic questions: *i*) how is this scenario compatible with the high- T_c superconductivity ($T_c \approx 40 \text{ K}$) in MgB_2 ; *ii*) at which extent MgB_2 is similar or differs from heavily doped semiconductors?

The trivial answer to the first question is the strong bidimensional character of the σ bands. Unlike three-dimensional systems, this yields a sizable, almost constant, density of states for n_{2D}^σ not too small, $N(\varepsilon) \sim 0.2 - 0.24 \text{ states/eV-cell}$ (summed over both spin and σ bands) for $n_{2D}^\sigma \gtrsim 0.02$ [67], and a finite electron–phonon coupling $\lambda \propto N(0)$. This situation makes a finite electron–phonon coupling compatible with a low carrier density and small Fermi energy, suggesting the onset of nonadiabatic effects as far as E_F becomes of the same order of the phonon frequencies ω_{ph} [39]. As a matter of fact, however, the comparison between the σ band Fermi energy $E_F^\sigma \approx 0.4 - 0.6 \text{ eV}$ and the frequency of the strongly coupled E_{2g} phonon mode $\omega_{\text{ph}} \sim 0.07 - 0.08 \text{ eV}$ [69, 70] leads to a relatively small nonadiabatic ratio $\omega_{\text{ph}}/E_F^\sigma \sim 0.1 - 0.2$. Although the nonadiabatic character can be enhanced by further reducing the charge carrier density, for instance upon atomic substitution in $\text{Mg}_{1-x}\text{Al}_x\text{B}_2$ or $\text{MgB}_{2-x}\text{C}_x$ alloys, nonadiabatic effects are expected to become more evident in the filling range where three-dimensional effects in the σ band dispersion become also important and the density of states is suppressed.

In order to answer the second question, it is worth to compare MgB_2 with graphite, where the σ bands lie $\sim 2 \text{ eV}$ below the Fermi level. As matter of principle, graphite would be a ideal candidate to reconcile finite density of states, low carrier density, small Fermi energy and sizable electron–phonon coupling if the chemical potential could be lowered enough to reach the σ bands. In the context of doped semiconductors outlined in Sec. 2.2, the chemical potential is usually tuned by the amount of doping. From the technical point of view, however, hole doping in graphite intercalated compounds is quite difficult and this task is unrealistic [71]. The case of MgB_2 shows an interesting alternative way, where a crucial role is played by the presence of the charged Mg layers. First principle calculations provide a useful tool to investigate the different role of the band filling (in the spirit of heavily doped semiconductors) and of the Mg layers, by comparing the band structure of MgB_2 with graphite and with a fictitious system $\square^{2+}\text{B}_2$ where charged Mg ions have been removed and replaced by a uniform charged background [67]. The band structure of $\square^{2+}\text{B}_2$ obeys in good approximation a rigid band model where the additional posi-

tive charges with respect to graphite are accommodated by a downward shift of the chemical potential which results in a hole filling of the π band. The peculiar role of the Mg layers in MgB_2 can be now pointed out by restoring the charged Mg ion in place of the uniform positive background. This leads to a relative upwards shift of the σ bands with respect to the π one, with a charge transfer from the π to the σ bands and with a resulting doping of the latter ones [67]. This scenario opens interesting perspectives in the search of new nonadiabatic materials based on the same principle, where the driving element is a partial charge transfer between some band structure, which plays the role of charge reservoir, and an almost filled (empty) bidimensional band.

4 Conclusions

The low charge carrier density is one of the most interesting features which is shared by different high- T_c superconductors. This is a quite puzzling feature since low carrier density is usually associated with bad metallic character, in contrast with the good superconducting properties of these materials. The small charge density has important consequences also on the electron–phonon interaction since the small Fermi energy E_F , intrinsically associated with the small charge density, may give rise to nonadiabatic electron–phonon effects as long as E_F becomes of the order of the phonon frequencies ω_{ph} . The onset of nonadiabatic effects has been proposed as a possible microscopic mechanism for the high- T_c superconductivity. In this scenario crucial ingredients are the small Fermi energy, the low charge density, a sizable electron density of states and electron–phonon matrix elements, a large Fermi surface.

In this contribution we have analyzed to a large extent the physical conditions which are required to reconcile all these elements in real materials. In particular we have shown that reconciling these all features requires peculiar conditions which go beyond the common picture of conventional metals. The specific cases of cuprates, fullerenes and MgB_2 have been discussed. We believe that a deeper understanding of the different ways this situation can be encountered in different materials can open new perspectives about the synthesis and optimization of new nonadiabatic high- T_c superconductors with low charge carrier density.

Acknowledgement This work was partially supported by the projects COFIN-2003 MIUR, FIRB RBAU017S8R and PRA-UMBRA INFM.

References

- [1] For a review on conventional low- T_c metals see: Superconductivity, edited by R. D. Parks (Dekker, New York, 1969).
- [2] P. W. Anderson and C. C. Yu, in: Highlights of Condensed Matter Theory, Proc. of the Int. School of Physics E. Fermi, LXXXIX, edited by F. Bassani and M. Tosi (North-Holland, New York, 1985).
- [3] P. B. Allen and B. Mitrovic, in: Solid State Physics, Vol. 37, edited by H. Ehrenreich, D. Turnbull, and F. Seitz (Academic Press, New York, 1982).
- [4] W. L. McMillan, Phys. Rev. **167**, 331 (1968).
- [5] J. G. Bednorz and K. A. Müller, Z. Phys. B **64**, 189 (1986).
- [6] L. C. Bourne, M. F. Crommie, A. Zettl, H. C. zur Loye, S. W. Keller, K. J. Leary, A. M. Stacy, K. J. Chang, and M. L. Cohen, Phys. Rev. Lett. **58**, 2337 (1987).
- [7] M. K. Crawford, W. E. Farneth, E. M. McCarron, R. L. Harlow, and E. H. Moudden, Science **250**, 1390 (1990).
- [8] J. P. Franck, S. Gygax, S. Soerensen, E. Altshuler, A. Hnatiw, J. Jang, M. A.-K. Mohamed, M. K. Yu, G. I. Sproule, J. Chrzanowski, and J. C. Irwin, Physica C **185–189**, 1379 (1991).
- [9] G. M. Zhao, M. B. Hunt, H. Keller, and K. A. Müller, Nature **385**, 236 (1997).
- [10] J. Hofer, K. Conder, T. Sasagawa, G. M. Zhao, M. Willemin, H. Keller, and K. Kishio, Phys. Rev. Lett. **84**, 4192 (2000).
- [11] R. Khasanov, D. G. Eshchenko, H. Luetkens, E. Morenzoni, T. Prokscha, A. Suter, N. Garifianov, M. Mali, J. Roos, K. Conder, and H. Keller, Phys. Rev. Lett. **92**, 057602 (2004).
- [12] C. Grimaldi, E. Cappelluti, and L. Pietronero, Europhys. Lett. **42**, 667 (1998).
- [13] A. S. Alexandrov, Europhys. Lett. **56**, 92 (2001).

- [14] A. Bill, V. Z. Kresin, and S. A. Wolf, *Phys. Rev. B* **57**, 10814 (1998).
- [15] T. Schneider and H. Keller, *Phys. Rev. Lett.* **86**, 4899 (2001).
- [16] A. Lanzara, P. V. Bogdanov, X. J. Zhou, S. A. Kellar, D. L. Feng, E. D. Lu, T. Yoshida, H. Eisaki, A. Fujimori, J.-I. Shimoyama, T. Noda, S. Uchida, Z. Hussain, and Z.-X. Shen, *Nature* **412**, 510 (2001).
- [17] G.-H. Gweon, T. Sasagawa, S. Y. Zhou, J. Graf, H. Takagi, D.-H. Lee, and A. Lanzara, *Nature* **430**, 187 (2004).
- [18] A. F. Hebard, M. J. Rosseinsky, R. C. Haddon, D. W. Murphy, S. H. Glarum, T. T. M. Palstra, A. P. Ramirez, and A. R. Kortan, *Nature* **350**, 600 (1991).
- [19] K. Tanigaki, T. W. Ebbesen, S. Saito, J. Mizuki, J. S. Tsai, Y. Kubo, and S. Kuroshima, *Nature* **352**, 222 (1991).
- [20] R. M. Fleming, A. P. Ramirez, M. J. Rosseinsky, D. W. Murphy, R. C. Haddon, S. M. Zahurak, and A. V. Makhija, *Nature* **352**, 787 (1991).
- [21] K. Holczer, O. Klein, S.-M. Huang, R. B. Kaner, K.-J. Fu, R. L. Whetten, and F. Diederich, *Science* **252**, 1154 (1991).
- [22] J. Nagamatsu, N. Nakagawa, T. Muranaka, Y. Zenitani, and J. Akimitsu, *Nature* **410**, 549 (2001).
- [23] Y. J. Uemura, G. M. Luke, B. J. Sternlieb, J. H. Brewer, J. F. Carolan, W. N. Hardy, R. Kadono, J. R. Kemp-ton, R. F. Kiefl, S. R. Kreitzman, P. Mulhern, T. M. Riseman, D. Li. Williams, B. X. Yang, S. Uchida, H. Takagi, J. Gopalakrishnan, A. W. Sleight, M. A. Subramanian, C. L. Chien, M. Z. Cieplak, G. Xiao, V. Y. Lee, B. W. Statt, C. E. Stronach, W. J. Kossler, and X. H. Yu, *Phys. Rev. Lett.* **62**, 2317 (1989).
- [24] Y. J. Uemura, L. P. Le, G. M. Luke, B. J. Sternlieb, W. D. Wu, J. H. Brewer, T. M. Riseman, C. L. Seaman, M. B. Maple, M. Ishitawa, D. G. Hinks, J. D. Jorgensen, G. Saito, and H. Yamochi, *Phys. Rev. Lett.* **66**, 2665 (1991).
- [25] *Polarons and Excitons*, edited by C. G. Kuper and G. D. Whitfield (Oliver and Boyd, Edinburgh, 1963).
- [26] A. S. Alexandrov and J. Ranninger, *Phys. Rev. B* **23**, 1796 (1981).
- [27] A. J. Millis, R. Mueller, and B. I. Shraiman, *Phys. Rev. B* **54**, 5389 (1996).
- [28] S. Ciuchi, F. de Pasquale, S. Fratini, and D. Feinberg, *Phys. Rev. B* **56**, 4494 (1997).
- [29] A. S. Alexandrov and N. Mott, *High Temperature Superconductors and Other Superfluids* (Taylor and Francis, London, 1994).
- [30] A. Deppeler and A. J. Millis, *Phys. Rev. B* **65**, 224301 (2002).
- [31] J. Mustre de Leon, R. de Coss, A. R. Bishop, and S. A. Trugman, *Phys. Rev. B* **59**, 8359 (1999).
- [32] E. V. L. de Mello and J. Ranninger, *Phys. Rev. B* **58**, 9098 (1998).
- [33] M. Tachiki, M. Machida, and T. Egami, *Phys. Rev. B* **67**, 174506 (2003).
- [34] A. Bussmann-Holder, A. R. Bishop, L. Genzel, and A. Simon, *Phys. Rev. B* **55**, 17151 (1997).
- [35] L. Pietronero, S. Strässler, and C. Grimaldi, *Phys. Rev. B* **52**, 10516 (1995).
- [36] C. Grimaldi, L. Pietronero, and S. Strässler, *Phys. Rev. B* **52**, 10530 (1995).
- [37] C. Grimaldi, L. Pietronero, and S. Strässler, *Phys. Rev. Lett.* **75**, 1158 (1995).
- [38] E. Cappelluti, C. Grimaldi, L. Pietronero, and S. Strässler, *Phys. Rev. Lett.* **85**, 4771 (2000).
- [39] E. Cappelluti, S. Ciuchi, C. Grimaldi, L. Pietronero, and S. Strässler, *Phys. Rev. Lett.* **88**, 117003 (2002).
- [40] L. Pietronero and S. Strässler, *Europhys. Lett.* **18**, 627 (1992).
- [41] E. Cappelluti and L. Pietronero, *Phys. Rev. B* **53**, 932 (1996).
- [42] E. Cappelluti and L. Pietronero, *Europhys. Lett.* **36**, 619 (1996).
- [43] A. Perali, C. Grimaldi, and L. Pietronero, *Phys. Rev. B* **58**, 5736 (1998).
- [44] E. Cappelluti, S. Ciuchi, C. Grimaldi, and L. Pietronero, *Phys. Rev. B* **68**, 174509 (2003).
- [45] I. G. Lang and Yu. A. Firsov, *Zh. Eksp. Teor. Fiz.* **43**, 1843 (1962) [*Sov. Phys. JETP*, 1301 (1963)].
- [46] C. Grimaldi, L. Pietronero, and M. Scattoni, *Eur. Phys. J. B* **10**, 247 (1999).
- [47] M. Scattoni, C. Grimaldi, and L. Pietronero, *Europhys. Lett.* **47**, 588 (1999).
- [48] E. Cappelluti, C. Grimaldi, and L. Pietronero, *Phys. Rev. B* **64**, 125104 (2001).
- [49] M. Botti, E. Cappelluti, C. Grimaldi, and L. Pietronero, *Phys. Rev. B* **66**, 054532 (2002).
- [50] For a comprehensive review about C₆₀ compounds see: O. Gunnarsson, *Rev. Mod. Phys.* **69**, 575 (1997).
W. E. Pickett, in *Solid State Physics*, Vol. 48, edited by H. Ehrenreich and F. Spaepen (Academic Press, New York, 1994).
- [51] S. Satpathy, *Chem. Phys. Lett.* **130**, 545 (1986).
- [52] S. Satpathy, V. P. Antropov, O. K. Andersen, O. Jepsen, O. Gunnarsson, and A. I. Liechtenstein, *Phys. Rev. B* **46**, 1773 (1992).
- [53] L. Pietronero, *Europhys. Lett.* **17**, 365 (1992).
- [54] N. M. Plakida, *High-Temperature Superconductivity* (Springer, Heidelberg, 1994).
- [55] W. E. Pickett, *Rev. Mod. Phys.* **61**, 433 (1989).
- [56] V. J. Emery, *Phys. Rev. Lett.* **58**, 2794 (1987).

- [57] C. M. Varma, S. Schmitt-Rink, and E. Abrahams, *Solid State Commun.* **62**, 681 (1987).
- [58] F. C. Zhang and T. M. Rice, *Phys. Rev. B* **41**, 7243 (1990).
- [59] H. Takagi, B. Batlogg, H. L. Kao, J. Kwo, R. J. Cava, J. J. Krajewski, and W. F. Peck Jr., *Phys. Rev. Lett.* **69**, 2975 (1992).
- [60] P. Fulde, *Electron Correlations in Molecules and Solids* (Springer, Heidelberg, 1995).
- [61] E. Dagotto, *Rev. Mod. Phys.* **66**, 763 (1994).
- [62] A. A. Abrikosov, L. P. Gorkov, and I. E. Dzyaloshinski, *Methods of Quantum Field Theory in Statistical Physics* (Dover, New York, 1975).
- [63] M. C. Gutzwiller, *Phys. Rev. Lett.* **10**, 159 (1963).
- [64] G. D. Mahan, *Many-Particle Physics* (Kluwer Academic, New York, 2000).
- [65] T. Yoshida, X. J. Zhou, T. Sasagawa, W. L. Yang, P. V. Bogdanov, A. Lanzara, Z. Hussain, T. Mizokawa, A. Fujimori, H. Eisaki, Z.-X. Shen, T. Kakeshita, and S. Uchida, *Phys. Rev. Lett.* **91**, 027001 (2003).
- [66] J. Kortus, I. I. Mazin, K. D. Belashchenko, V. P. Antropov, and L. L. Boyer, *Phys. Rev. Lett.* **86**, 4656 (2001).
- [67] J. M. An and W. E. Pickett, *Phys. Rev. Lett.* **86**, 4366 (2001).
- [68] K. Papagelis, J. Arvanitidis, K. Prassides, A. Schenck, T. Takenobu, and Y. Iwasa, *Europhys. Lett.* **61**, 254 (2003).
- [69] Y. Kong, O. V. Dolgov, O. Jepsen, and O. K. Andersen, *Phys. Rev. B* **64**, 020501 (2001).
- [70] K.-P. Bohnen, R. Heid, and B. Renker, *Phys. Rev. Lett.* **86**, 5771 (2001).
- [71] For a review about graphite and graphite intercalated compounds see: M. S. Dresselhaus and G. Dresselhaus, *Adv. Phys.* **30**, 139 (1981).